

Full structure determination of an alkali-metal/CO coadsorption phase for Co{10 $\bar{1}$ 0}-c(2 \times 2)-(K+CO)

P. Kaukasoina and M. Lindroos

Department of Physics, Tampere University of Technology, P.O. Box 692, FIN-33101 Tampere, Finland

P. Hu and D. A. King

Department of Chemistry, University of Cambridge, Lensfield Road, Cambridge CB2 1EW, United Kingdom

C. J. Barnes

School of Chemical Sciences, Dublin City University, Glasnevin, Dublin 9, Ireland

(Received 28 October 1994; revised manuscript received 1 March 1995)

A structural analysis of a c(2 \times 2)-(K+CO) coadsorption phase on Co{10 $\bar{1}$ 0} by low-energy electron diffraction has yielded a full picture of the geometry of a model alkali-metal CO coadsorption system. Potassium atoms are located in fourfold hollow sites above second-layer Co atoms, and CO molecules are displaced by 0.5 ± 0.2 Å from the high-symmetry Co short bridge sites near the center of gravity of the three neighboring K adatoms. The CO causes a substantial increase, by 0.4 Å, in the K-Co nearest-neighbor bond length, and K adatoms are located with their centers above the O atoms in the neighboring CO. This has important implications for the bonding interactions within the adlayer.

I. INTRODUCTION

Coadsorption of potassium and CO has served as a prototype to examine the interaction of electropositive atoms with molecular adsorbates. Despite the use of almost every surface-sensitive technique to examine the alkali-metal CO interaction, a basic understanding of potassium/CO bonding is lacking.¹ This has stemmed in a large part from an absence of a quantitative knowledge of the adlayer geometry. Usually these systems do not exhibit long-range order, and the small number of systems which have an ordered overlayer have large unit cells which prohibit full structural analysis by low-energy electron diffraction, at the present time.

Recently an adsorption microcalorimeter has been deployed to study CO+K coadsorption, on Ni{100}.² The CO adsorption heat is increased from 123 kJ mol⁻¹ on the clean surface to 170 kJ mol⁻¹ for low precoverages of K, but with high K precoverages the CO adsorption heat is increased to ~ 300 kJ mol⁻¹. These results were interpreted in terms of formation of K^{δ+}CO^{δ-} islands.

A range of other models had been previously suggested, including formation of polymeric (CO)_y⁻ anions stabilized by alkali cations often termed salt formation,³ rehybridization of molecular CO to an sp² configuration,⁴⁻⁶ a direct interaction between the potassium 4s/4p resonance with the CO 1π states,^{7,8} and an ionic model involving complete charge transfer from the potassium 4s to the CO 2π* levels yielding a CO⁻K⁺ ionic salt.⁹⁻¹¹ There remains extensive debate regarding the correct description of the alkali-metal/CO interaction. A number of studies have indicated that the CO molecule remains upright or close to upright in the coadsorbed phases, which appears to eliminate the polymeric salt model, which involves C—O bond axes oriented at a considerable angle from the surface normal. Of the other

candidates, the sp² rehybridization model of Weimer and co-workers,⁴⁻⁶ based on the observation of a split 1π level in ultraviolet photoemission spectroscopy (UPS), would require a marked increase in the CO bond length seen by comparing it to carbonyl cluster compounds. This would also seem unlikely as near-edge x-ray-absorption fine-structure (NEXAFS) results indicate only a moderate increase in the interatomic distance induced by K coadsorption.¹²⁻¹⁴ The favored models to date would seem to be the direct 1π-alkali bonding interaction of Eberhardt *et al.*,⁷ which geometrically requires the alkali-metal adsorbate to straddle the carbon-oxygen for optimal interaction, and that of Schultz,¹ involving formation of ionic islands due to complete charge transfer from the potassium valence level to the CO 2π* orbital leading to a K⁺CO⁻ ionic layer. The latter model is able to explain a large number of the observed properties of alkali-metal CO coadsorption systems including the large reduction (by several hundred wave numbers) of the CO internal stretching frequency, increase in the C—O bond length, the alkali-metal-induced increase in the adsorption energy of CO, and the related stabilization of potassium due to the increased ionicity. In particular, this model is able to explain qualitatively the shift to lower energy of potassium core levels due to the electrostatic stabilization of the final-state core hole by surrounding CO anions.

Coadsorption of potassium and CO on a hcp Co{10 $\bar{1}$ 0} surface provides a rather unique opportunity for a complex structure determination. The adsorption of potassium on this surface has been carefully studied by Barnes¹⁵ and Masuda.¹⁶ In particular, at a potassium coverage of exactly 0.5 ML a c(2 \times 2) overlayer is formed, which a dynamic low-energy electron-diffraction (LEED) *I(V)* analysis revealed as a potassium overlayer above an essentially unreconstructed Co{10 $\bar{1}$ 0} surface. Adatoms

are located in the $[\bar{1}2\bar{1}0]$ channels directly above nearest-neighbor second-layer cobalt atoms, with an effective potassium radius intermediate between that of ionic (1.33 Å) and metallic (2.26 Å) potassium of 1.87 ± 0.05 Å. Saturation of this layer with CO at 300 K leads to a very well-ordered $c(2 \times 2)$ coadsorbed layer with a K:CO stoichiometry at or close to 1:1.¹⁷ Thus the system provides an ideal candidate to study quantitatively the full geometric structure surrounding both potassium and CO adatoms.

II. EXPERIMENT

The evaporation rate of potassium was calibrated by LEED utilizing the previous observation that in the potassium coverage range $0.58 \geq \Theta_K \geq 0.30$ ML a split $c(2 \times 2)$ LEED pattern is formed with a perfect $c(2 \times 2)$ being formed in an extremely narrow coverage range of (0.5 ± 0.03) ML.¹⁶ The coadsorption phase was formed by saturation of the $c(2 \times 2)$ -K overlayer with CO at room temperature. The $c(2 \times 2)$ -(K+CO) overlayer exhibited bright sharp fractional-order beams. Previous studies of K/CO coadsorption on $\text{Co}\{10\bar{1}0\}$ indicated that the diffracted intensity in the fractional-order beams arises solely from a $c(2 \times 2)$ -(K+CO) coadsorption phase; no domains of $c(2 \times 2)$ -K remain. This can be demonstrated by comparison of $I(V)$ spectra of the $c(2 \times 2)$ -K and $c(2 \times 2)$ -(K+CO) phases. Intense peaks from the pure $c(2 \times 2)$ -K phase fall in minima in the measured $c(2 \times 2)$ -(K+CO) spectra, and inspection clearly demonstrates that any remaining areas of $c(2 \times 2)$ -K are negligibly small.

To reduce data collection time to a minimum, the variation of intensity with energy over a range 40–300 eV of all beams was acquired simultaneously by recording the pattern on video tape using a video recorder. Symmetrically equivalent beams were averaged to reduce residual sample misalignment, and normalized to constant primary beam current. Careful checks were made to ensure that electron-beam damage was minimal by rescanning $I(V)$ spectra as a function of time. It appeared that coadsorption of CO with K rendered the molecular CO significantly less susceptible to electron-beam damage compared to CO on clean $\text{Co}\{10\bar{1}0\}$, where several minutes exposure led to severe damage. All $I(V)$ spectra were recorded with the sample at or just above room temperature.

III. COMPUTATIONS

Theoretical $I(V)$ spectra were calculated using the dynamic LEED package of Van Hove and Tong.¹⁸ The muffin-tin potentials for cobalt and potassium were taken from Moruzzi, Janak, and Williams.¹⁹ Phase shifts for carbon monoxide come from Tong *et al.*²⁰ The energy-independent imaginary part of the inner potential was -4 eV, and Debye temperatures were 385, 200, 843, and 1405 K for Co, K, O, and C, respectively. The real part of the inner potential was varied in the R -factor analysis.

In the case of bulk $\text{Co}\{10\bar{1}0\}$, atomic layers are separated by alternate short (0.724 Å) and long (1.447 Å) spacings. The layers separated by short spacings were

treated as composite layers, and calculation of scattering matrices was performed using the combined space method for composite layers by matrix inversion. The same method was also used when calculating the scattering matrices for the overlayer if the corresponding interlayer spacings were short. The scattering between layers was accomplished stacking layers by layer doubling.

Calculated and measured $I(V)$ curves were compared using the Pendry R factor.²¹ Having found the best structure, all geometrical parameters were individually varied, and curves of the R factor as a function of the geometric variables were obtained. The uncertainties of the parameters were then obtained using the variance of the Pendry R factor.²¹

IV. RESULTS

For the $\text{hcp}\{10\bar{1}0\}$ surface, the crystal could be terminated by the short or long interlayer distance, or a mixture of both terminations separated by diatomic steps. As in previous studies for clean $\text{Co}\{10\bar{1}0\}$ -(1×1) (Refs. 22 and 23) and $\text{Co}\{10\bar{1}0\}$ - $c(2 \times 2)$ -K,¹⁵ where the surface was shown to be uniquely terminated by a short interlayer spacing, only that termination was considered here. Twelve different model geometries were tested, as shown in Fig. 1. These models split naturally into four subgroups, with potassium situated at high-symmetry sites including on-top, fourfold hollow, and long or short bridge sites. In each of the four cases carbon monoxide can be situated at two different high-symmetry sites, both of which are in the middle of two potassium atoms. In addition, another CO adsorption site was considered for all four potassium sites, in which CO was situated at the middle of the triangle formed by three surrounding potassium atoms. Additional studies were also performed assuming substitutional sites for K in Co rows. These

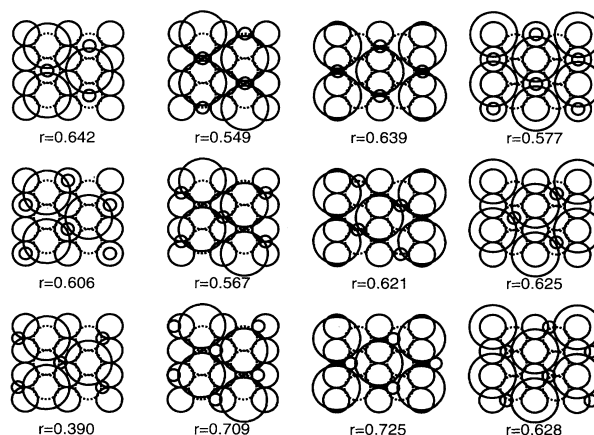


FIG. 1. The model geometries and corresponding lowest Pendry R factors after the first scan of structural parameters. The large circles correspond to potassium atoms and the small circles are the CO molecules. The first- (second-) layer Co atoms are represented as solid (dotted) circles of medium size.

structures were excluded from the full treatment because of inferior R factors. The possibility of two CO molecules per one K atom in the favored model was similarly excluded.

The interlayer spacings of the cobalt substrate were initially frozen at the bulk values, and only the heights of potassium, carbon, and oxygen were varied over a wide range in steps of 0.05 \AA . The lowest R factors obtained are shown in Fig. 1 for individual model geometries. The model with the best R factor consisted of potassium located in the fourfold hollow site with carbon monoxide situated at the center of gravity of the three neighboring potassium atoms. The other model geometries must be ruled out because of their markedly larger R factors. After full optimization of the best model, the minimum Pendry R factor was 0.316. The geometrical parameters and the corresponding uncertainties are shown in Fig. 2, while the optimal theory-experiment agreement is illustrated in Fig. 3. The potassium-cobalt nearest-neighbor bond length is $3.51 \pm 0.11 \text{ \AA}$, which gives an effective potassium radius of $2.26 \pm 0.11 \text{ \AA}$, being the same as the bulk value of metallic potassium (2.26 \AA) (the ionic radius is 1.33 \AA). The carbon-oxygen bond length is $1.20 \pm 0.08 \text{ \AA}$. This value is larger than that previously determined by LEED on a range of transition-metal surfaces by about 0.07 \AA .²⁴ The optimum R factor was obtained when carbon monoxide was slightly tilted from the upright orientation, but the uncertainty of the lateral po-

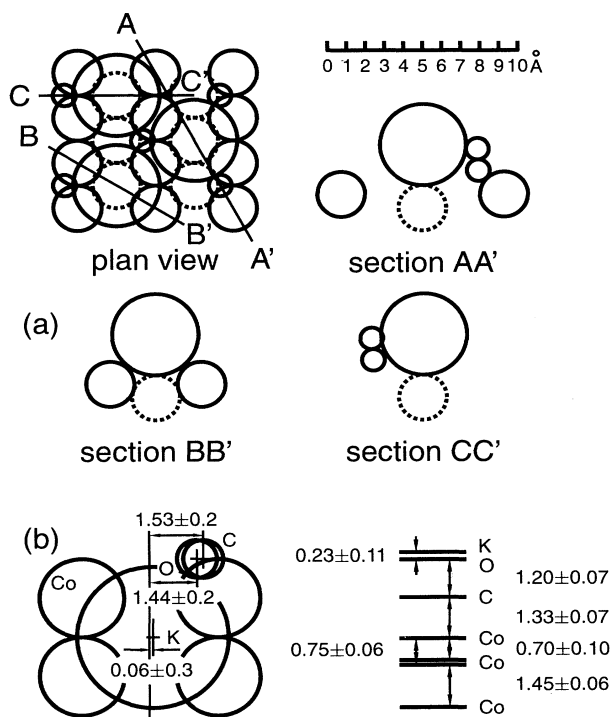


FIG. 2. (a) Top and side views of the favored geometric structure, and (b) optimal geometric parameters with associated uncertainties in \AA .

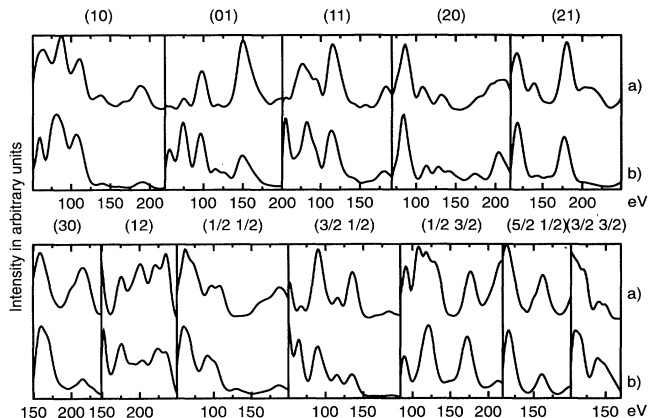


FIG. 3. Optimal theory-experiment agreement for all beams. (a) Calculated and (b) measured intensities as functions of electron energy.

sition yields a large uncertainty in the tilt angle of $4^\circ \pm 10^\circ$. The CO molecules tilt in the $[0001]$ azimuth between the two neighboring potassium atoms in the $[1\bar{2}10]$ channels. The carbon atoms are laterally displaced by 0.12 \AA from the center of gravity of three neighboring potassium atoms, or, equivalently, displaced from the short bridge sites by $0.50 \pm 0.2 \text{ \AA}$. The carbon atoms were located $1.33 \pm 0.07 \text{ \AA}$ above the center of gravity of the outermost cobalt layer, resulting in a carbon-cobalt bond length of 1.90 \AA . Subtraction of the cobalt metallic radius from this value yields an effective carbon radius of 0.64 \AA which compares with average values of 0.58 , 0.62 , and 0.67 \AA for on-top, bridge, and fcc hollow sites for CO on clean metal surfaces.²⁴ The value for the $\text{Co}\{10\bar{1}0\}-c(2 \times 2)-(\text{K} + \text{CO})$ system is thus quite in line with the displaced bridge site determined. The potassium layer is $0.23 \pm 0.11 \text{ \AA}$ above the oxygen layer.

Adsorbate-induced reconstruction of the cobalt selvedge was considered in the form of buckling of the second cobalt layer. The center of gravity of the outermost two cobalt layers was allowed to shift. A slight buckling of $0.05 \pm 0.09 \text{ \AA}$ of the second layer has been detected with the second-layer atoms directly beneath top-layer potassium being shifted downwards. The optimal first (short) interlayer spacing was found to be $0.70 \pm 0.06 \text{ \AA}$, corresponding to a small inward relaxation of -3.3% . The second (long) interlayer spacing optimized at $1.45 \pm 0.06 \text{ \AA}$, virtually identical to that of bulk $\text{Co}\{10\bar{1}0\}$ (1.447 \AA).

Figure 4 illustrates the sensitivity of the analysis to various aspects of the geometry, including the potassium-oxygen interplanar separation, the carbon-oxygen bond length, and the lateral position of carbon. These curves are illustrated in the form of response of the Pendry R factor to a single geometric parameter with all other variables fixed.

Many of the geometrical findings are in line with previ-

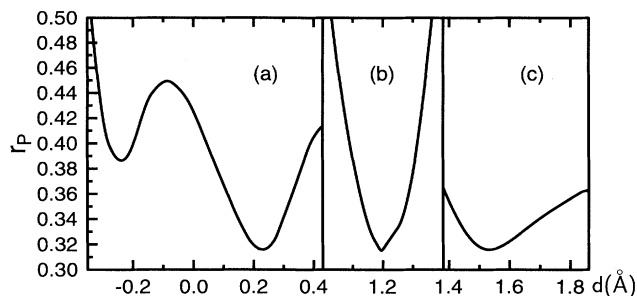


FIG. 4. The Pendry R factor for the optimal structure as a function of (a) separation between K and O layers, (b) CO bond length, and (c) lateral position of carbon, while other parameters are kept constant.

ous expectations of alkali-metal/CO systems in the high-alkali-metal coverage regime. The CO molecule is found to be oriented in an upright or close to upright configuration, which rules out a number of previously proposed models of the alkali-metal/CO interaction including the salt model of Lackey *et al.*³ which necessarily requires the carbon-oxygen bond axis to be oriented far from the surface normal in the polymeric squarate anions. Other models involving lying down or strongly reoriented Co can likewise be excluded.²⁵ Although no quantitative structural determinations for the carbon-oxygen bond length have to date been performed for CO on Co{10 $\bar{1}$ 0}, based on a range of quantitative structural studies on low-index fcc and hcp surfaces an increase in the intramolecular bond length of between 0.05 and 0.10 Å may be inferred. This observation is in keeping with the general picture of alkali-metal-induced increased back donation into the $2\pi^*$ antibonding molecular orbital of CO within the Blyholder model.²⁶

Perhaps the most surprising result is the observed large shift of potassium *away* from the cobalt surface with the potassium adatoms being located *above* the oxygen of CO. This leads to an increase in the effective potassium radius from 1.87 ± 0.05 Å for the $c(2 \times 2)$ potassium overlayer to 2.26 ± 0.11 Å in the coadsorbed phase. Thus models involving a direct interaction between the occupied 1π CO orbitals with the $4s/4p$ resonance in potassium would seem unlikely to be the dominant factors in the bonding of coadsorbed layers, as the electron density of the 1π orbitals straddles the carbon-oxygen bond.⁷

V. DISCUSSION

No CO-induced site switching of the potassium equilibrium site occurs, allowing potassium to remain in the energetically favored [1 $\bar{2}$ 10] channels and the CO to bond close to the close-packed cobalt [1 $\bar{2}$ 10] rows, again as favored for CO on clean Co{10 $\bar{1}$ 0}. A reflection-

absorption infrared spectroscopy (RAIRS) analysis indicates both on-top and bridge sites as occupied on clean Co{10 $\bar{1}$ 0}, depending on coverage. At a CO fractional coverage of 0.5 in the absence of K, a $p(2 \times 1)$ structure is formed, with all CO molecules in atop positions and $\nu_{\text{CO}} = 2020 \text{ cm}^{-1}$.²⁷ The CO therefore *does* undergo site switching in the K coadsorption $c(2 \times 2)$ structure.

The most interesting aspect of the geometry is the large increase in the nearest-neighbor K—Co bond length of 0.4 Å, leaving the potassium nucleus 0.23 Å *above* the oxygen atoms in the CO molecule; i.e., potassium is far from straddling the C—O bond as assumed by both Schultz and co-workers in the ionic model^{9,10} and Eberhardt *et al.*⁷ in the $1\pi/4s,4p$ direct interaction. This observation would tend to legislate against the $1\pi/4s$ direct interaction being the *major* component of the alkali-metal K/CO bonding. However, it would be unwise to rule out this possibility completely. Nevertheless, such a large movement of the alkali-metal atom away from the cobalt substrate must necessarily imply a considerable decrease in the metal-potassium component of the adsorption energy. It is clear from adsorption calorimetry,² and a common feature of all alkali-metal/CO systems, that the potassium binding is actually *increased*. Naturally the loss of metal-alkali bonding must be compensated for by an increased lateral attractive interaction with chemisorbed CO. We would stress that the structure has a distinctly unexpected feature; that is, the proximity of the K adatom to three O atoms. As shown in Fig. 2, this is a chemical bonding distance.

Given the determined geometry, it would seem likely that the gain in K/CO bonding arises partly from an ionic contribution due to the interaction of functionally positively charged potassium ($\text{K}^{\delta+}$) with the net negatively charged $\text{CO}^{\delta-}$. Direct experimental evidence of increased back donation of charge into the $2\pi^*$ resonance straddling the Fermi level comes from the increased intermolecular bond length and the decreased frequency of the internal mode of the molecule. However, the lowering of the CO stretching frequency does not seem to imply *complete* charge transfer. The redshift observed in RAIRS to 1730 cm^{-1} (Ref. 27) must have components of the downward shift due to the increased effective coordination as the CO moves from an atop site toward a hollow site, along with the Stark shift due to the electrostatic field in the coadsorbed layer. It is therefore surprising that the shift is so small, particularly given the proximity of K to CO in this structure. That excess net positive charge is located on potassium in coadsorption systems is evident from the decrease in work function obtained on CO coadsorption.

In order to test such a model quantitatively, a first-principle total-energy calculation should be performed. The starting geometry of the structure obtained here could be input, and the energy locally minimized around this structural model. Such a calculation, in tandem with calculations of a $c(2 \times 2)$ -K overlayer on Co{10 $\bar{1}$ 0} and a 0.5-ML $p(2 \times 1)$ CO overlayer, would provide the missing link regarding the valence charge reorganization to finally confirm which model (or indeed hybrid of models) correctly describes the K/CO interaction in the high-

coverage limit.

We are aware of two other structural analyses of alkali-metal + CO systems. Davis *et al.* have studied using photoelectron diffraction Ni{111}(2×2)-K+2CO,²⁸ and Over *et al.* have performed a LEED intensity analysis of Ru{0001}(2×2)-Cs+CO.²⁹

ACKNOWLEDGMENTS

P.K. and M.L. would like to acknowledge the Academy of Finland for financial support. The U.K. SERC is acknowledged for an equipment grant, and the Oppenheimer Trust for financial support to P.H.

-
- ¹P. A. Schultz, *J. Vac. Sci. Technol. A* **8**, 2425 (1990).
²N. Al-Sarraf, J. T. Stuckless, and D. A. King, *Nature* **360**, 243 (1992).
³D. Lackey *et al.*, *Surf. Sci.* **152/153**, 513 (1985).
⁴J. J. Weimer, E. Umbach, and D. Menzel, *Surf. Sci.* **155**, 132 (1985).
⁵J. J. Weimer and E. Umbach, *Phys. Rev. B* **30**, 4863 (1984).
⁶J. J. Weimer, E. Umbach, and D. Menzel, *Surf. Sci.* **159**, 83 (1985).
⁷W. Eberhardt *et al.*, *Phys. Rev. Lett.* **54**, 1856 (1985).
⁸W. Eberhardt *et al.*, *Chem. Phys. Lett.* **124**, 237 (1986).
⁹P. A. Schultz, *J. Vac. Sci. Technol. A* **5**, 1061 (1987).
¹⁰P. A. Schultz and R. P. Messmer, *Surf. Sci.* **209**, 229 (1989).
¹¹D. R. Jennison, *J. Vac. Sci. Technol. A* **5**, 684 (1987).
¹²F. Sette *et al.*, *Phys. Rev. Lett.* **54**, 935 (1985).
¹³W. Wurth *et al.*, *Phys. Rev. B* **34**, 1336 (1986).
¹⁴M. Gleeson *et al.*, *Surf. Sci.* (to be published).
¹⁵C. J. Barnes *et al.*, *Surf. Sci.* **251/252**, 561 (1991).
¹⁶T. Masuda *et al.*, *Surf. Sci.* **276**, 122 (1992).
¹⁷C. J. Barnes and M. Valden, *J. Phys. Condens. Matter* **1**, SB185 (1989).
¹⁸M. A. Van Hove and S. Y. Tong, *Surface Crystallography by LEED*, Springer Series in Chemical Physics Vol. 2 (Springer-Verlag, Berlin, 1979).
¹⁹Y. Moruzzi, J. Janak, and A. Williams, *Calculated Electronic Properties of Metals* (Pergamon, New York, 1978).
²⁰S. Y. Tong *et al.*, *Surf. Sci.* **94**, 73 (1980).
²¹J. B. Pendry, *J. Phys. C* **13**, 937 (1980).
²²M. Lindroos *et al.*, *Chem. Phys. Lett.* **173**, 92 (1990).
²³H. Over *et al.*, *Surf. Sci. Lett.* **254**, L469 (1991).
²⁴H. Ohtani, M. A. Van Hove, and G. A. Somorjai, *The Structure of Surfaces II*, Springer Series in Surface Sciences Vol. 11 (Springer-Verlag, Berlin, 1988), pp. 219–224.
²⁵H. P. Bonzel, *Surf. Sci. Rep.* **8**, 43 (1988).
²⁶G. Blyholder, *J. Phys. Chem.* **68**, 2772 (1964).
²⁷R. L. Toomes and D. A. King (unpublished).
²⁸R. Davis *et al.*, *Phys. Rev. Lett.* **74**, 1621 (1995).
²⁹H. Over *et al.*, *Phys. Rev. B* **51**, 4661 (1995).